Journal of Photochemistry and Photobiology A: Chemistry 207 (2009) 167–172

Contents lists available at ScienceDirect

Journal of Photochemistry and Photobiology A: Chemistry

journal homepage: www.elsevier.com/locate/jphotochem

Methylene blue–calixarenesulfonate supramolecular complexes and aggregates in aqueous solutions

Olívia Varga[a], Miklós Kubinyi[a,b,*], Tamás Vidóczy[a], Péter Baranyai[a], István Bitter[a,c], Mihály Kállay[b]

[a] Chemical Research Center, Hungarian Academy of Sciences, P.O. Box 17, 1525 Budapest, Hungary
[b] Department of Physical Chemistry and Materials Science, Budapest University of Technology and Economics, 1521 Budapest, Hungary
[c] Department of Organic Chemistry and Technology, Budapest University of Technology and Economics, 1521 Budapest, Hungary

ARTICLE INFO

Article history:
Received 18 March 2009
Received in revised form 4 June 2009
Accepted 3 July 2009
Available online 5 August 2009

Keywords:
Calixarene
Supramolecular complex
Aggregation
Fluorescence quantum yield
Triplet lifetime
Electron transfer

ABSTRACT

The complexation of methylene blue (**MB**) by calix[*n*]arenesulfonates (**SCA*n***, *n* = 4, 6, 8) was studied in aqueous solutions with various ionic strengths, using absorption and fluorescence spectroscopy and laser flash photolysis. The simultaneous reactions **MB** + **SCA*n*** ↔ **MB**·**SCA*n*** (1) and **MB**·**SCA*n*** + **MB** ↔ **MB$_2$**·**SCA*n*** (2) were observed. The equilibrium constants $K(1)$ and $K(2)$ are high (10^5–10^7), their dependence on the ionic strength can be described by the extended Debye–Hückel law. $K(2) > K(1)$ for all the three systems, in accord with the strongly aggregating nature of **MB**. In **MB**–**SCA8** mixtures complexes with more than two **MB** units were also detected. The fluorescence of the dye is partially or completely quenched in the complexes, the formation of triplet state complexed **MB** cations is negligible. At low **SCA*n*** concentrations and ionic strengths the formation of colloidal aggregates was detected by resonance Rayleigh scattering.

1. Introduction

The thiazine dye methylene blue (**MB** in Fig. 1) has many applications. It is a commonly used cellular stain, a textile dye in industry and a redox indicator. Besides, **MB** is frequently employed as a spectroscopic probe. In particular, its adsorption on minerals [1] and its binding to RNA [2], DNA [3] and proteins [4,5] attract considerable research interest. **MB** also has important medical applications: it is used as sensitizer in photodynamic therapy of cancer [6], and as sensitizer for photodynamic antimicrobial chemotherapy [7,8]. An important feature of **MB** is the formation of aggregates in water even at relatively low concentrations, which has to be taken into account in the above applications.

The effects of the local environment on the aggregation and/or on the redox properties of **MB** were studied in cyclodextrin [9,10] and in cucurbituril [11] supramolecular complexes as model systems. In our present work the interaction of **MB** with calix[*n*]arenesulfonates (**SCA*n*** in Fig. 1, *n* = 4, 6, 8) has been investigated. Whereas in cyclodextrin and cucurbituril complexes the dye cation guest is partly embedded in a hydrophobic cavity, calixarenesulfonates represent environments with high negative charge density. The optical spectroscopic features of calixarenes and their complexes, involving various calixarene–dye complexes are summarized in a recent review by Mohammed-Ziegler and Billes [12].

In our previous study we found that oxazine 1 (**OX**), a cationic dye with low dimerization affinity forms a 1:1 and a 2:1 complex complex with **SCA8** (**OX**:**SCA8**) [13]. In the present work our goal has been to describe the changes in the photophysical properties of a chemically similar, but easily aggregating dye, **MB**, induced by the supramolecular interaction with the multiply charged **SCA*n*** hosts. We applied stationary absorption and fluorescence spectroscopy and – with respect to the significance of triplet states in the medical applications – laser flash photolysis as experimental methods. A qualitative analysis of the visible absorption spectra of **MB**–**SCA*n*** (*n* = 4, 6) supramolecular systems indicated the occurrence of a 1:1 complex and of **MB** dimer in aqueous solutions [14]. The absorption spectra of these systems in methanol–water mixtures suggested the presence of complexes with 1:1 and 1:2 stoichiometry (**MB**:**SCA*n***, *n* = 4, 6, 8) [15].

We performed a detailed quantitative analysis of the spectral data yielding the spectra of the **MB**–**SCA*n*** complexes and the equilibrium constants characterizing their stability. These results might have some practical importance, since many supramolecular systems consisting of a macrocyclic host and a fluorescent dye guest can be applied in competitive fluorescent techniques [16–18]. The principle of these techniques is that the analyte, which is a non-fluorescent compound, or has a fluorescence spectrum not sensitive to complexation, expels the fluorescent host from the complex.

* Corresponding author at: Chemical Research Center, Hungarian Academy of Sciences, P.O. Box 17, 1525 Budapest, Hungary. Tel.: +36 1 438 1120.
E-mail address: kubinyi@chemres.hu (M. Kubinyi).

1010-6030/$ – see front matter © 2009 Elsevier B.V. All rights reserved.
doi:10.1016/j.jphotochem.2009.07.001

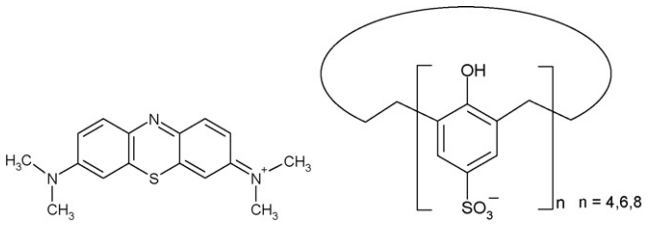

Fig. 1. Structures of methylene blue cation (**MB**) and calixarenesulfonate anions (**SCA*n***).

2. Materials and methods

MB (chloride salt) was purchased from Fluka. The syntheses of the three calixarenesulfonate sodium salts was described in our previous work [13]. Their purity was checked by electrospray ionization mass spectrometry and no impurity was detected. (Before the mass spectrometric measurements the Na^+ ions were removed from the samples by consecutive ion exchange steps.)

The initial concentration of **MB** in the samples used for the absorption and fluorescence spectroscopic measurements was 4×10^{-6} and 2×10^{-6} M, respectively, that of the sulfocalixarenes was varied from 0 to 10^{-4} M. The measurements were carried out in phosphate buffer medium (to avoid the uncertainties arising from the presence of different metal ions, the buffer was made of Na_2HPO_4 and NaH_2PO_4). The ionic strengths of the solutions was set by the addition of NaCl. Since **MB** strongly adsorbs on glass/water interface [19], the stock solutions and the **MB–SCA*n*** mixtures were prepared in polypropylene vessels. The mixtures were kept for 1 day before measuring the spectra.

All the spectroscopic measurements were carried out at 25 °C. UV–vis absorption spectra were recorded on an Agilent 8453 spectrophotometer. Fluorescence spectra were taken by using a

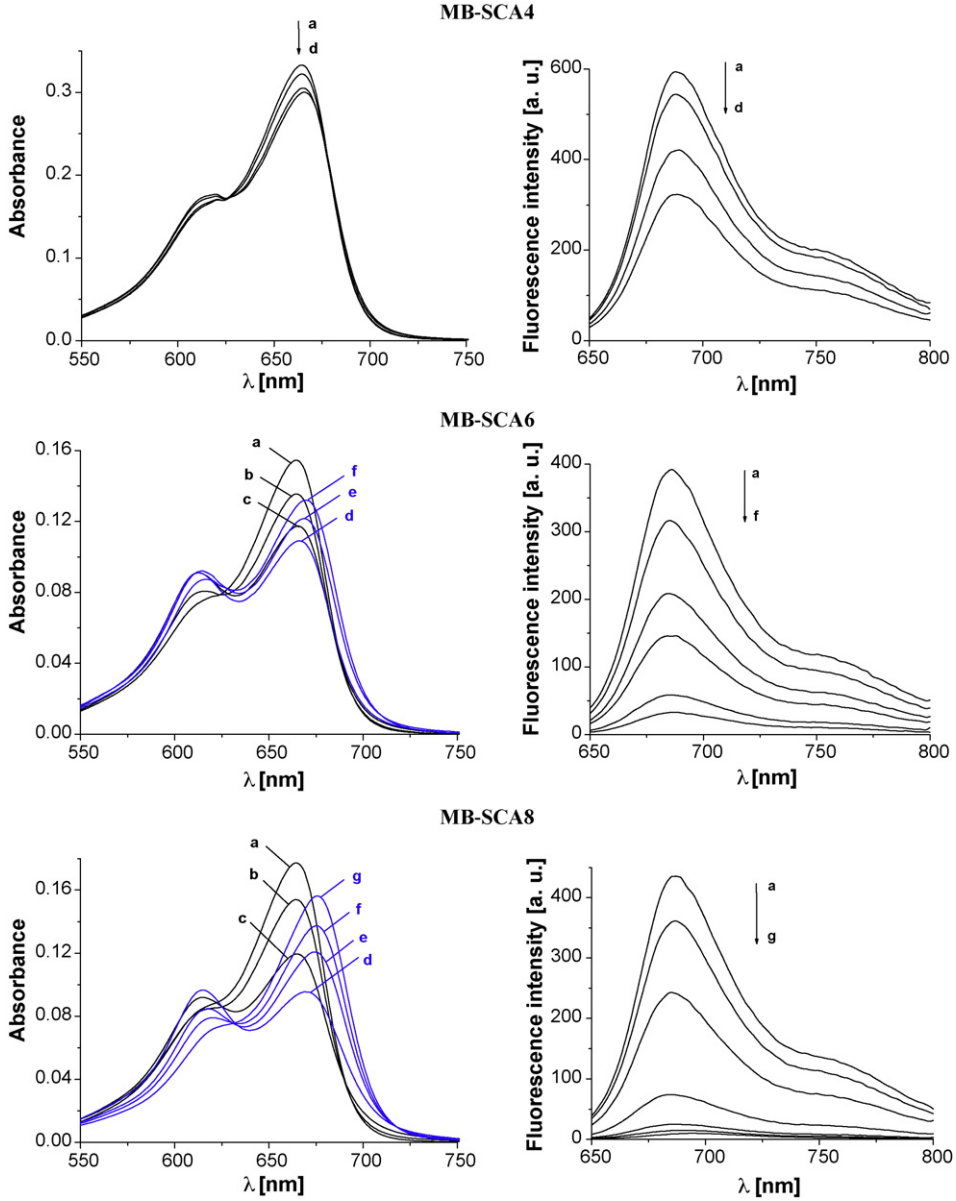

Fig. 2. Absorption and fluorescence spectra of **MB–SCA*n*** mixtures. *Concentrations*: **MB–SCA4** (pH 5.3, $I = 1.6 \times 10^{-2}$ M) $[MB]_0 = 4 \times 10^{-6}$ M, $[SCA4]_0$ = (a) 0 M, (b) 2.2×10^{-6} M, (c) 1×10^{-5} M, (d) 2.2×10^{-5} M; **MB–SCA6** (pH 7.4, $I = 8.2 \times 10^{-3}$ M) $[MB]_0 = 2 \times 10^{-6}$ M, $[SCA6]_0$ = (a) 0 M, (b) 1×10^{-6} M, (c) 4.6×10^{-6} M, (d) 1×10^{-5} M, (e) 4.6×10^{-5} M, (f) 1×10^{-4} M; **MB–SCA8** (pH 6.5, $I = 8.2 \times 10^{-3}$ M) $[MB]_0 = 2 \times 10^{-6}$ M, $[SCA8]_0$ = (a) 0 M, (b) 1×10^{-7} M, (c) 4.6×10^{-7} M, (d) 2.2×10^{-6} M, (e) 1×10^{-5} M, (f) 2.2×10^{-5} M, (g) 1×10^{-4} M.

Perkin-Elmer LS 50B spectrofluorimeter, with the excitation wavelength set to 627 nm where the absorbance of **MB** changed relatively little upon the addition of **SCA*n***-s in different concentrations. The fluorescence quantum yield of **MB** was determined using cresyl violet as standard [20]. The resonance Rayleigh scattering experiments were performed on the same spectrofluorimeter.

The transient absorption decays of **MB** and its mixtures with **SCA*n***-s were measured using a laser flash photolysis setup equipped with a Nd^{3+}-YAG Q-switched laser [21]. The excitation wavelength was 532 nm (the second harmonic of the laser).

3. Results and discussion

3.1. Spectra of supramolecular systems

The self-aggregation of **MB** in the 2×10^{-6} or 4×10^{-6} M solutions without **SCA*n***-s was considered negligible on the basis of the results of preliminary measurements when absorption spectra were taken from solutions containing **MB** in various concentrations, with pH and ionic strength (I) values applied in the further experiments. The absorbance vs. concentration plots for these samples were found linear up to 10^{-5} M. We note that the molar absorption coefficient and the fluorescence quantum yield data for **MB** dissolved in water, reported in earlier studies vary in a relatively large range. Our results are in good agreement to those published by Atherton and Harriman [22].

The phenolic protons of Na-calixarenesulfonates dissociate in consecutive steps. For **SCA4** $pK_{a1} = 3.26$, $pK_{a2} = 11.8$ [23]. The pH values of the **MB**–**SCA4** solutions were set to 5.3, where **SCA4** was present in its singly deprotonated form. The pK_a values for the first three deprotonations of **SCA6** are 2.7, 5.0 and ~12 [24], the corresponding values for **SCA8** are 3.73, 4.39 and 8.07 [25]. We selected the pH values of 7.4 and 6.5 for the **MB**–**SCA6** and **MB**–**SCA8** mixtures, respectively, in which the doubly deprotonated forms of the respective calixarenes were predominant.

The stoichiometries and the spectra of the complexes, and the equilibrium constants for the complex formation reactions were determined by an analysis of the experimental spectra obtained from sets of solutions. In each set the concentration of **MB** and the ionic strength were held at a constant value, meanwhile the concentration of the calixarene was varied. (The sets consisted of 11 samples: 1 neat **MB** solution and 10 **MB**–**SCA*n*** mixtures.)

The changes in the absorption and fluorescence spectra of **MB**, generated by the addition of **SCA4**, **SCA6** and **SCA8** are illustrated in Fig. 2. (For sake of clarity not all the spectra measured at the given pH and I values are shown.)

The absorption spectrum of pure **MB** in the visible range is characterized by a band at 664.5 nm ($\varepsilon = 84{,}500\ M^{-1}\ cm^{-1}$) with a shoulder at 610 nm, which are assigned to the S_0–S_1 transition of n–π^* character, and to its 0–1 vibronic transition, respectively [26]. The addition of **SCA6** and **SCA8** leads to marked changes: the spectral features of pure **MB** are gradually replaced by two separate bands, one band at somewhat lower wavelengths than the shoulder in the spectrum of **MB**, the other band at somewhat higher wavelengths than the absorption maximum of the dye. The variations in the spectra of **MB**–**SCA4** mixtures are much less pronounced. There is no isobestic point in the absorbance spectra of the **MB**–**SCA*n*** solutions, indicating that **MB** is present in at least three different forms in these systems.

MB is a weakly fluorescent dye, we measured the value of 0.020 ± 0.002 for its fluorescence quantum yield in pure water. The fluorescence band of pure **MB** falls to 687 nm with a shoulder at 750 nm. As is shown in Fig. 2, the addition of the three calixarenes results in fluorescence quenching, but the overall shape of the band and the position of the maximum remain almost unchanged.

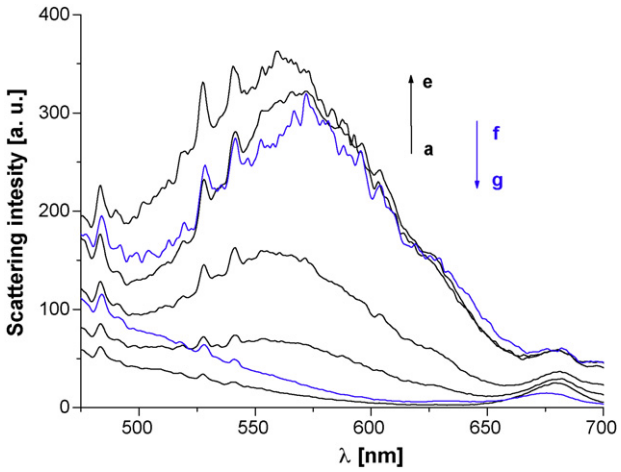

Fig. 3. Rayleigh scattering spectra of **MB**–**SCA8** mixtures (pH 6.5, $I = 8.2 \times 10^{-3}$ M). *Concentrations*: $[MB]_0 = 7 \times 10^{-6}$ M, $[SCA8]_0$ = (a) 0 M, (b) 10^{-7} M, (c) 2×10^{-7} M, (d) 5×10^{-7} M, (e) 7×10^{-7} M, (f) 10^{-6} M, (g) 2×10^{-6} M.

The presence of colloidal aggregates was demonstrated by resonance Rayleigh scattering (RRS) measurements. The **MB**–**SCA6** and **MB**–**SCA8** mixtures with **MB** concentrations 4×10^{-6} M or lower, which were used in the absorption and fluorescence spectroscopic experiments, exhibited no sign of aggregation. Above this concentration the addition of small amounts of calixarenes to the **MB** solution resulted in the formation of colloidal aggregates, as was indicated by the appearance of a band around 560 nm (see Fig. 3). A signal at similar position was observed in the RRS spectra of **MB**–chondroitine 4-sulfate systems [27]. In case of our **MB**–**SCA*n*** systems the RRS signal had a maximum intensity at a given **SCA*n*** concentration. As can be seen in Fig. 3, this is around a concentration ratio of 10:1 (**MB**:**SCA8**), where the opposite charges of the **MB** and **SCA8** ions practically compensate each other.

3.2. Analysis of experimental spectra

The number of the components in the individual supramolecular systems, which absorb in the visible range were assessed by rank analysis (i.e. the number of significant singular values of the matrix built from all measured data). The analysis indicated the occurrence of three absorbing species, which were presumed to be uncomplexed **MB**, **MB**·**SCA*n*** and $\mathbf{MB_2}$·**SCA*n***, and the reaction scheme

$$\mathbf{MB} + \mathbf{SCA}n \overset{K_1}{\rightleftharpoons} \mathbf{MB} \cdot \mathbf{SCA}n, \tag{1a}$$

$$\mathbf{MB} \cdot \mathbf{SCA}n + \mathbf{MB} \overset{K_2}{\rightleftharpoons} \mathbf{MB_2} \cdot \mathbf{SCA}n \tag{1b}$$

was applied, where K_1 and K_2 are the apparent equilibrium constants

$$K_1 = \frac{[\mathrm{MB} \cdot \mathrm{SCA}n]}{[\mathrm{MB}] \cdot [\mathrm{SCA}n]}, \tag{2a}$$

$$K_2 = \frac{[\mathrm{MB_2} \cdot \mathrm{SCA}n]}{[\mathrm{MB} \cdot \mathrm{SCA}n] \cdot [\mathrm{MB}]}. \tag{2b}$$

The material balance equations for the host and guest compounds are

$$[\mathrm{MB}]_0 = [\mathrm{MB}] + [\mathrm{MB} \cdot \mathrm{SCA}n] + 2[\mathrm{MB_2} \cdot \mathrm{SCA}n] \tag{3}$$

and

$$[\mathrm{SCA}n]_0 = [\mathrm{SCA}n] + [\mathrm{MB} \cdot \mathrm{SCA}n] + [\mathrm{MB_2} \cdot \mathrm{SCA}n]. \tag{4}$$

The values of K_1 and K_2 and the spectra of the two complexes have been calculated in a similar dual iteration as in Ref. [13]. In

each outer loop of the iteration new values were given to K_1 and K_2 and the equilibrium concentrations, [MB], [SCA*n*], [MB·SCA*n*] and [MB_2·SCA*n*] in the individual samples with total concentrations of $[MB]_0$ and $[SCAn]_0$ were calculated, solving the system of Eqs. (2a), (2b), (3) and (4). This was followed by the calculation of the spectra, which were taken as sums of the contributions of the uncomplexed and the two complexed forms of **MB**, i.e. the absorbance of the *i*th sample at the *j*th wavelength was expressed as

$$A_i^j(\text{cacd}) = (\varepsilon^j_{MB} \cdot [MB]_i + \varepsilon^j_{MB\cdot SCAn} \cdot [MB \cdot SCAn]_i + \varepsilon^j_{MB_2\cdot SCAn} \cdot [MB_2 \cdot SCAn]_i) \cdot \ell, \quad (5)$$

where ε^j_{MB}, $\varepsilon^j_{MB\cdot SCAn}$ and $\varepsilon^j_{MB_2\cdot SCAn}$ denote absorption coefficients, ℓ is the length of the optical path. ε^j_{MB} was known from the spectrum of pure **MB**, $\varepsilon^j_{MB\cdot SCAn}$ and $\varepsilon^j_{MB_2\cdot SCAn}$ were determined in an inner loop of iteration, by a least-square fitting of these values to the measured absorbances.

The scheme involving the formation of only a 1:1 and a 2:1 **MB**:**SCA*n*** complex was found suitable for the description of all the **MB–SCA6** systems and most of the **MB–SCA8** systems studied. (At the end of the dual iteration the average deviations between the experimental and calculated absorbance values in the individual spectra were typically 0.0004–0.0005, the highest deviations were 0.001–0.002, even the latter figures are well within the accuracy of the spectrometer.) In case of the **MB–SCA8** mixtures with lower ionic strengths and low **SCA8** concentrations the rank analysis suggested the presence of further components, without giving a reliable estimation for their number. These components are presumably calixarenes binding more than two **MB** units. Attempts were made to analyze the experimental spectra of these systems assuming the simultaneous formation of further complexes, **MB_m·SCA8**, with $m > 2$, these calculations, however, produced unreliable results due to the large number of independent parameters (equilibrium constants and absorption coefficients).

It was attempted to interpret the absorption spectral data of the **MB–SCA4** mixtures also in terms of the formation of a 1:1 and a 2:1 complex. Only the spectra measured at $I = 1.6 \times 10^{-2}$ M were analyzed, since at lower ionic strengths strong aggregation occurred, resulting in poorly reproducible results, at higher I values the spectral variations upon the addition **SCA4** were still smaller. The rank analysis suggested the occurrence of three species absorbing in the visible range also in this system. However, the spectra of the **MB–SCA4** complexes could not be determined reliably even from these data, since the differences among the experimental absorbance values proved to be too small even in this case. Considering the close similarity of the spectra of the **MB_2·SCA6** and **MB_2·SCA8** complexes, and of the spectra of the **MB·SCA6** and **MB·SCA8** complexes (see Fig. 4), it may be assumed that the **MB–SCA4** complexes have spectra similar to those of the corresponding **MB** complexes of the larger calixarenesulfonates. Thus, estimated values for K_1 and K_2 of the **MB–SCA4** systems were calculated taking the absorption coefficients for **MB_2·SCA4** and **MB·SCA4** in Eq. (5) from the spectra of **MB_2·SCA6** and **MB·SCA6**, respectively. The values of the average and highest deviations (0.003 and 0.007 absorbance units, respectively) suggested that this model was reasonable.

The fluorescence spectra, in which the addition of calixarenes is accompanied by quenching, but not by clear changes in the position or the shape of the band, are less informative on the composition of the **MB–SCA*n*** supramolecular systems. Therefore, an independent determination of the equilibrium constants from the fluorescence data was not attempted.

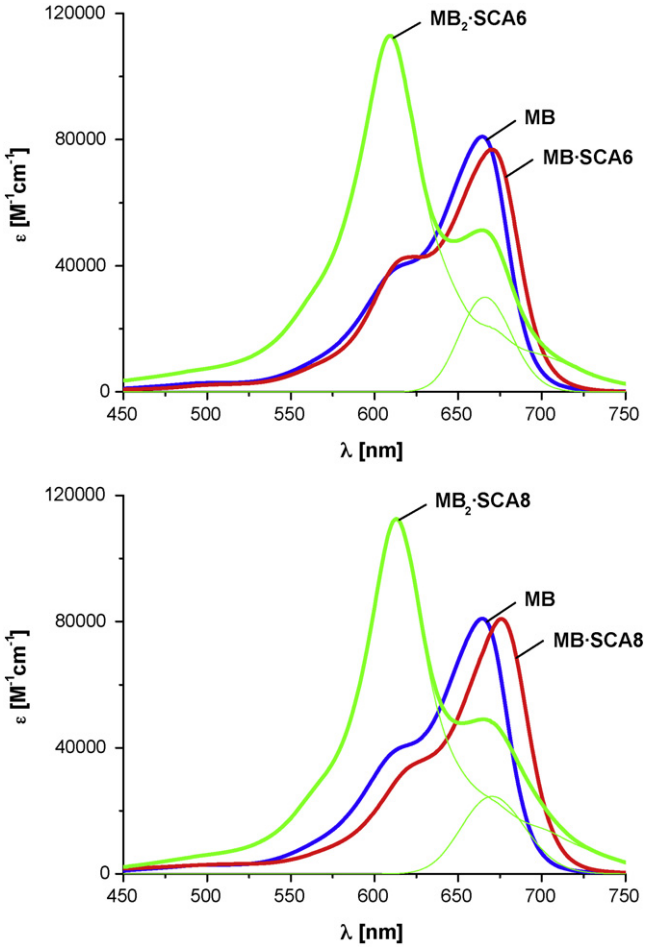

Fig. 4. Absorption spectra of **MB–SCA6** and **MB–SCA8** complexes. The thin traces show the decomposition of the spectra of the **MB_2·SCA*n*** complexes into the spectra of complexed 'H'-type dimer (sum of two Gaussians) and 'J'-type dimer (one Gaussian).

3.3. Spectra and structure of complexes

The spectra of the complexes obtained in the calculations are displayed in Fig. 4.

The formation of 1:1 complexes (**MB·SCA6**, **MB·SCA8**) is accompanied only by minor changes in the absorption spectrum of **MB**, like a small shift of the visible band to the red. The two bands in the spectra of the 2:1 complexes (**MB_2·SCA6**, **MB_2·SCA8**) can be assigned to two different complexed forms of the **MB_2** dimer. The spectra of dye dimers can be discussed qualitatively on the basis of the exciton splitting theory, which relates the spectral properties to the mutual orientation of the constituents [28]. In brief, the ground state of the dimer, S_0 is doubly degenerate, whereas the excited state of the dimer splits into a higher and a lower energy state, S_1' and S_1'', respectively. Considering the spectra of the two simplest dimer models with parallel transition moments, for the 'H-type' (sandwich-like) dimer only the transition into the higher energy state is allowed, whereas for the 'J-type' (head-to-tail aligned) dimer only the excitation into the lower energy state. On this ground, the stronger blue-shifted components around 610 nm are attributable to complexed H-type dimers, whereas the weaker features around 670 nm may be assigned to complexed J-type dimers. As comparison, in the spectrum of **MB** in aqueous solution the H-type dimer gives rise to a strong band at 605 nm, whereas the absorption of the J-type dimer is weak and almost coincides with the band of the monomer form [29,30].

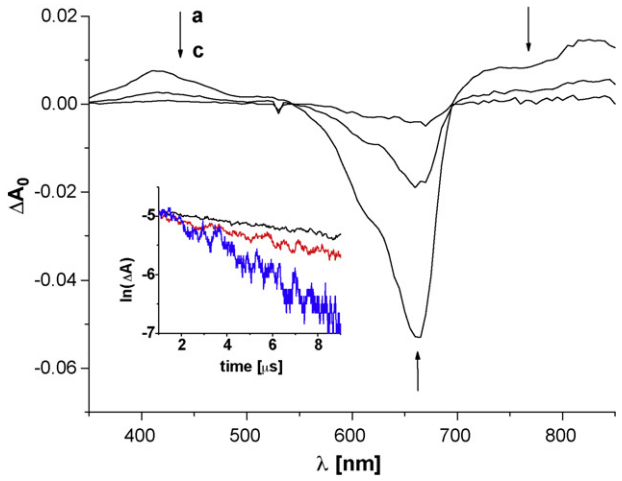

Fig. 5. Triplet absorption spectra of **MB–SCA6** mixtures (pH 7.4, $I = 8.2 \times 10^{-3}$ M). *Concentrations*: $[MB]_0 = 4 \times 10^{-6}$ M, $[SCA6]_0$ = (a) 0 M, (b) 1×10^{-5} M, (c) 1×10^{-4} M. The inset shows logaritmic plots of triplet decay curves. *Concentrations*: $[MB]_0 = 4 \times 10^{-6}$ M, $[SCA6]_0$ = (black) 0 M, (red) 4.6×10^{-6} M, (blue) 2.2×10^{-5} M. (For interpretation of the references to color in this figure legend, the reader is referred to the web version of the article.)

The fluorescence intensities of the complexes were calculated from the experimental fluorescence spectra of the mixtures, taking the concentrations of the uncomplexed and complexed forms of **MB** from the analysis of the absorption spectra. The 1:1 complexes were found non-fluorescent, whereas the 2:1 complexes proved to be fluorescent with intensities of 0.3–0.5 related to the intensity of the pure dye. Since by Kasha's rule fluorescence is expected only from the lowest excited energy levels (in this case from S_1''), H-type dimers are expected to be dark, and the same applies to the **MB–SCA*n*** complexes involving H-type dimers. The fact that the 2:1 complexes are fluorescent, confirms the occurrence of dimers with structures different from H-type alignment.

3.4. Triplet state of *MB*

The flash photolysis experiments were carried out with **MB–SCA6** and **MB–SCA8** systems of 8.2×10^{-3} M ionic strength. The transient absorption spectra (the ΔA_0 zero-time signals as functions of wavelengths) obtained for pure **MB** and two **MB–SCA6** solutions are compared in Fig. 5. The positive band at 415 nm derives from the triplet absorption of **MB**, the negative band at 665 nm arises from the depletion of the S_0 state of the dye ("bleaching"). The intensity of these bands decreases as the concentration of the calixarene is increased, but no new features attributable to the complexes appear. The ΔA_0 values measured at 415 nm were plotted against the free **MB** concentrations, [MB] in the individual **MB–SCA6** mixtures, taking the latter data from the previously described analysis of the absorption spectra. ΔA_0 is very low as [MB] approaches zero, i.e. at high **SCA6** contents, and the plot is closely linear, confirming that the triplet absorption arises solely from the pure dye.

The decay curves of these mixtures measured at the peaks of the above positive and negative bands could be described by a single exponential in good approximation (see the inset in Fig. 5). In pure water the triplet lifetime of 90 ± 2 μs was measured for **MB**, somewhat longer than the value reported by Gak et al. [31]. This lifetime shortened in the buffers applied (e.g. to 23.1 μs in the buffer with pH 7.4, $I = 8.2 \times 10^{-3}$ M). It decreased further in the presence of calixarenes, which is a measure of dynamic quenching by the added calixarene salts. The quenching rate constants are 8×10^9 and 1.6×10^{10} M^{-1} s^{-1} for **SCA6** and **SCA8**, respectively.

The mechanism of triplet quenching cannot be energy transfer from **MB** to calixarene because the triplet energy of **MB** is very low ($\Delta E_{00} = 138$ kJ/mol) [32]. The Gibbs energy (ΔG°) of the photoinduced electron transfer from the phenolate parts of the calixarenes (two phenolic OH groups are deprotonated) can be calculated from the Rehm–Weller equation:

$$\Delta G'^\circ = e\left[E^0(\mathrm{PhO^\bullet/PhO^-}) - E^0(\mathrm{MB/MB^\bullet})\right] - \Delta E_{00} + w, \quad (6)$$

where w is the Coulombic term which can be neglected in a highly polar solvent. The redox potential of the **MB**/**MB•** couple is −0.23 V vs. normal hydrogen electrode (NHE) [33]. Redox potentials are not available for calixarenes, for a rough estimation we can consider 0.86 V vs. NHE for a phenolate anion [34,35]. The calculated ΔG° value (−33 kJ/mol) supports a very efficient photoinduced electron transfer process as a mechanism for triplet quenching.

3.5. Equilibrium constants

The apparent equilibrium constants (2a) and (2b) are related to the K^0 'true' equilibrium constants (expressed with activities) as

$$\log K = \log K^0 + \log \gamma_G + \log \gamma_H - \log \gamma_{G\cdot H}, \quad (7)$$

where γ_G, γ_H, and $\gamma_{G\cdot H}$ are the activity coefficients of the guest (**MB**), of the host (**SCA*n***) in reaction (1a), **MB**·**SCA*n*** in reaction (1b)) and of the product. For supramolecular systems consisting of a charged guest, a multiply charged macrocyclic host and their complex(es), the dependence of the activity coefficients on the ionic strength can be described by a modified form of the Debye–Hückel equation:

$$\log \gamma_i = -z_i^2 \frac{AI^{1/2}}{1 + I^{1/2}}, \quad (8)$$

where z_i is the 'effective charge' of the respective species: z_G and z_H represent the portions of the charged functional groups of the guest and the host, taking part in the binding process, the effective charge of the complex can be taken as $z_{G\cdot H} = z_G + z_H$ [36,37]; $A = 0.5112$ for aqueous solutions at 25 °C. Substituting (8) into (7) yields

$$\log K = \log K^0 - 2|z_G z_H| \frac{AI^{1/2}}{1 + I^{1/2}}. \quad (9)$$

Adapting this approach to our systems

$$\log K_1 = \log K_1^0 - 2|z_{MB} z_{SCAn}| \frac{AI^{1/2}}{1 + I^{1/2}} \quad (10a)$$

and

$$\log K_2 = \log K_2^0 - 2|z_{MB} z_{MB\cdot SCAn}| \frac{AI^{1/2}}{1 + I^{1/2}}. \quad (10b)$$

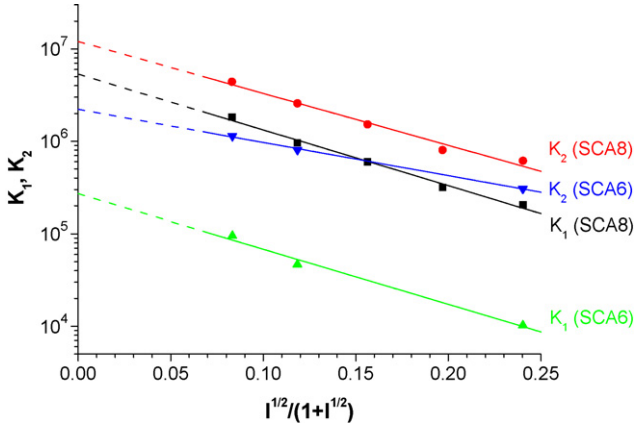

Fig. 6. Debye–Hückel plots of the equilibrium constants of reactions in **MB–SCA6** and **MB–SCA8** systems.

The Debye plots for the equilibrium constants of the **MB**–**SCA*n*** systems are displayed in Fig. 6. The $\log K$ data fit well to the four trend lines. The values of the equilibrium constants extrapolated to $I = 0$ are $K_1^0 = 2.7 \times 10^5$ M, $K_2^0 = 2.2 \times 10^6$ M for the **MB**–**SCA6** and $K_1^0 = 5.3 \times 10^6$ M, $K_2^0 = 1.2 \times 10^7$ M for the **MB**–**SCA8** system. Presuming that the effective charge of the dye cation, $z_{MB} = +1$, the effective charges of $z_{SCA6} = -5.8$, $z_{MB \cdot SCA6} = -3.5$, $z_{SCA8} = -5.9$, $z_{MB \cdot SCA8} = -5.5$ are obtained for the multiply charged host anions from the slopes of the trend lines.

For the **MB**–**SCA4** systems with $I = 1.6 \times 10^{-2}$ the calculations described in Chapter 3.2 yielded the significantly lower equilibrium constants $K_1 = 2.3 \times 10^4$ and $K_2 = 1.2 \times 10^5$ M.

4. Conclusions

MB forms 1:1 and 2:1 complexes with **SCA*n***-s containing $n = 4$, 6 and 8 calixarene units, in **MB**–**SCA8** mixtures complexes with more than two **MB** units also occur. The results clearly indicate that the complexes are held together primarily by electrostatic forces: (1) the values of the K_1 and K_2 association constants are higher by several orders of magnitudes than those measured for the reactions of cationic dye guests with neutral hosts; (2) the dependence of K_1 and K_2 on the ionic strength follows the Debye–Hückel law; (3) the complexation of **MB** by **SCA*n***-s leads to fluorescence quenching, unlike its complexation by neutral hosts, where the hydrophobic nature of the environment results in fluorescence enhancement.

The fact that $K_2 > K_1$, i.e. the binding of a free guest by an 1:1 complex is preferred to its binding by a free host can be explained by the strongly aggregating nature of the **MB** guest. The strong affinity for dimerization in environments with negative local charges is a characteristic feature of **MB**, which can be utilized in material science. The phenomenon was observed on glass/water interface [19,38], at aqueous micelle interfaces using anionic tenzide [39,40] and in bacterial suspensions [41]. Dimer **MB** is formed together with higher aggregates on layered silicates [1,42] and on ice crystallites [43]. Our results on the behavior of **MB** in the presence of **SCA*n*** hosts, representing an environment with high negative charge density may help to understand better the information obtainable with help of this spectral dye probe on more complex materials systems.

Acknowledgements

Financial support has been provided by the European Research Council (ERC) under the European Community's Seventh Framework Programme (FP7/2007-2013), ERC Grant Agreement no. 200639, and by the Hungarian Scientific Research Fund (OTKA, Grant no. NF72194). Mihály Kállay acknowledges the Bolyai Research Scholarship of the Hungarian Academy of Sciences. The authors are grateful to Dr. Kornél Nagy for the mass spectrometric measurements.

References

[1] K. Yurekli, E. Conley, R. Krishnamoorti, Langmuir 21 (2005) 5825–5830.
[2] R. Sinha, M.M. Islam, K. Bhadra, G.S. Kumar, A. Banerjee, M. Maiti, Bioorg. Med. Chem. 14 (2006) 800–814.
[3] Y. Wang, A. Zhou, J. Photochem. Photobiol. A 190 (2007) 121–127.
[4] J.A. Bartlett, G.L. Indig, Photochem. Photobiol. 70 (1999) 490–498.
[5] Y.-J. Hu, Y. Liu, R.-M. Zhao, J.-X. Dong, S.-S. Qu, J. Photochem. Photobiol. A 179 (2006) 324–329.
[6] J.P. Tardivo, A. Del Giglio, C.S. de Oliveira, D.S. Gabrielli, H.C. Junqueira, D.B. Tada, D. Severino, R. de Fatima Turchiello, M.S. Baptista, Photodiagn. Photodyn. Ther. 2 (2005) 175–191.
[7] M. Wainwright, Photochem. Photobiol. Sci. 3 (2004) 406–411.
[8] C.M. Cassidy, M.M. Tunney, P.A. McCarron, R.F. Donnelly, J. Photochem. Photobiol. B 95 (2009) 71–80.
[9] C. Lee, Y.W. Sung, J.W. Park, J. Phys. Chem. B 103 (1999) 893–898.
[10] G. Zhang, S. Shuang, C. Dong, J. Pan, Spectrochim. Acta A 59 (2003) 2935–2941.
[11] P. Montes-Navajas, A. Corma, H. Garcia, ChemPhysChem 9 (2008) 713–720.
[12] I. Mohammed-Ziegler, F. Billes, J. Incl. Phenom. Macrocycl. Chem. 58 (2007) 19–42.
[13] M. Kubinyi, T. Vidóczy, O. Varga, K. Nagy, I. Bitter, Appl. Spectrosc. 59 (2005) 134–139.
[14] Q. Lu, J. Gu, H. Yu, C. Liu, L. Wang, Y. Zhou, Spectrochim. Acta A 68 (2007) 15–20.
[15] Y. Sueishi, N. Inazumi, T. Hanaya, J. Phys. Org. Chem. 18 (2005) 448–455.
[16] X.S. Zhu, J. Sun, J. Wu, Talanta 72 (2007) 237–242.
[17] A. Praetorius, D.M. Bailey, T. Schwarzlose, W.M. Nau, Org. Lett. 10 (2008) 4089–4092.
[18] N. Korbakov, P. Timmerman, N. Lidich, B. Urbach, A. Sa'ar, S. Yitzchaik, Langmuir 24 (2008) 2580–2587.
[19] N. Matsuda, J.J. Zheng, D.K. Qing, A. Takatsu, K. Kato, Appl. Spectrosc. 57 (2003) 100–103.
[20] D. Magde, J.H. Brannon, T.L. Cremers, J. Olmsted, J. Phys. Chem. 83 (1979) 696–699.
[21] Z. Katona, A. Grofcsik, P. Baranyai, I. Bitter, G. Grabner, M. Kubinyi, T. Vidóczy, J. Mol. Struct. 450 (1998) 41–45.
[22] S.J. Atherton, A. Harriman, J. Am. Chem. Soc. 115 (1993) 1816–1822.
[23] I. Yoshida, N. Yamammoto, F. Sagara, D. Ishii, K. Ueno, S. Shinkai, Bull. Chem. Soc. Jpn. 65 (1992) 1012–1015.
[24] K. Suga, T. Ohzono, M. Negishi, K. Deuchi, Y. Morita, Supramol. Sci. 5 (1998) 9–14.
[25] M. Sonoda, K. Hayashi, M. Nishida, D. Ishii, I. Yoshida, Anal. Sci. 14 (1998) 493–499.
[26] G.N. Lewis, O. Goldschmid, T.T. Magel, J. Bigeleisen, J. Am. Chem. Soc. 65 (1943) 1150–1154.
[27] L. Zhang, N. Li, F. Zhao, K. Li, Anal. Sci. 20 (2004) 445–450.
[28] K. Kemnitz, N. Tamai, I. Yamazaki, N. Nakashima, K. Yoshihara, J. Phys. Chem. 90 (1986) 5094–5101.
[29] L. Antonov, G. Gergov, V. Petrov, M. Kubista, J. Nygren, Talanta 49 (1999) 99–106.
[30] K. Patil, R. Pawar, P. Talap, Phys. Chem. Chem. Phys. 2 (2000) 4313–4317.
[31] V.Y. Gak, V.A. Nadtochenko, J. Kiwi, J. Photochem. Photobiol. A 116 (1998) 57–62.
[32] S.L. Murov, I. Carmichael, G.L. Hug, Handbook of Photochemistry, 2nd ed., Marcel Dekker, New York, 1993.
[33] T. Ohno, N.N. Lichtin, J. Am. Chem. Soc. 102 (1980) 4636–4643.
[34] C. Li, M.Z. Hoffman, J. Phys. Chem. B 103 (1999) 6653–6656.
[35] K. Lang, P. Kubát, P. Lhoták, J. Mosinger, D.M. Wagnerová, Photochem. Photobiol. 74 (2001) 558–565.
[36] H.J. Schneider, R. Kramer, S. Simova, U. Schneider, J. Am. Chem. Soc. 110 (1988) 6442–6448.
[37] M.A.S. Hossain, H.J. Schneider, Chem. Eur. J. 5 (1999) 1284–1290.
[38] K. Fujita, K. Taniguchi, H. Ohno, Talanta 65 (2005) 1066–1070.
[39] M.K. Carroll, M.A. Unger, A.M. Leach, M.J. Morris, C.M. Ingersoll, F.V. Bright, Appl. Spectrosc. 53 (1999) 780–784.
[40] H.C. Junqueira, D. Severino, L.G. Dias, M.S. Gugliotti, M.S. Baptista, Phys. Chem. Chem. Phys. 4 (2002) 2320–2328.
[41] M.N. Usacheva, M.C. Teichert, M.A. Biel, J. Photochem. Photobiol. B 71 (2003) 87–98.
[42] A. Czimerova, J. Bujdak, A. Gaplovsky, Colloids Surf. A 243 (2004) 89–96.
[43] D. Heger, J. Jirkovsky, P. Klan, J. Phys. Chem. A 109 (2005) 6702–6709.